



FORESTRY SCIENCE

Landsat data respond to variations in the structure of Caatinga plant communities along a successional gradient

FERNANDA KELLY G. DA SILVA, FERNANDO ROBERTO MARTINS, ADUNIAS DOS SANTOS TEIXEIRA, JEAN-FRANÇOIS MAS, BRUNO S. DE MENEZES, FLAVIO JORGE PONZONI & FRANCISCA S. DE ARAÚJO

Abstract: Plant community succession is generally approached with phytosociological methods, but field surveys are time-consuming, expensive, and limited to several of sites. Remote sensing offers an efficient and economical way to analyze vegetation on large extensions and in inaccessible areas. Most studies addressing remote sensing and tree community succession refer to forest physiognomies. We investigated whether structural changes that occur in non-forest physiognomies are identified by multispectral sensor images (OLI-Landsat). Thirteen 0.1-ha plots were set up in Caatinga fragments aging 10-15, 20-25, 30-35, 40-45 and >50 years to calculate the total density of individuals (TD), mean canopy height (H), total basal area (G) and total aboveground biomass (AGB). We performed correlation analyses between these structural descriptors and eight remote sensing variables (reflectance data and spectral indices) obtained from Landsat images at the end of the rainy season and during the dry season. Blue and short-wave infrared reflectances were negatively correlated with mean height, basal area and biomass, regardless of the analyzed scene (coefficients between -0.58 and -0.79). The litter layer (a non-photosynthetic vegetation component) and the soil exposure are important factors influencing the spectral data.

Key words: ecological succession, Landsat, phytosociology, remote sensing, semiarid.

INTRODUCTION

Approximately two-thirds of the global forest area are classified as secondary forests (Mackey et al. 2015). In the tropics, secondary forests cover about 70% of all forest area (FAO 2010) and are, therefore, more common than primary forests. Secondary forests represent a potential carbon sink and result from natural or man-made disturbances (Pain et al. 2021), triggering ecological succession, which consists of changes in the community structure and species composition over time (Clements 1916, Pickett et al. 2011).

The usual way to characterize the plant communities successional process has been applying phytosociological methods. Still, field surveys are time-consuming, costly, and limited to a small number of landscape sites (Clark et al. 2004, Song et al. 2007, Timothy et al. 2016). On the other hand, Remote sensing potentially offers an efficient and economical way to analyze vegetation on large extensions and in inaccessible areas (Timothy et al. 2016, Chambers et al. 2007). However, estimating attributes of plant communities using remote sensing poses some difficulties, such as vegetation physiognomy, structure and phenology, sensor

characteristics (spatial, radiometric, and spectral resolution, for example), geometric factors (angles of illumination and sight, for example), among others (Franklin 2001, Ponzoni & Rezende 2004, Ponzoni et al. 2012, Barbosa et al. 2014).

To understand the potential of remote sensing in the characterization of succession in plant communities, several studies have been carried out, especially in tropical rainforests (Mausel et al. 1993, Lucas et al. 2000, Steininger 2000, Vieira et al. 2003, Clark et al. 2004, Lu et al. 2004, Ponzoni & Rezende 2004, Arroyo-Mora et al. 2005, Feeley et al. 2005, Castillo et al. 2012, Gallardo-Cruz et al. 2012, Martinuzzi et al. 2012, Yang et al. 2012, Galvão et al. 2015). A considerable part of these studies has related remotely-sensed data with attributes measured in the field, enabling an ecological understanding of the spectral dynamics of vegetation. Chronosequence studies in Amazon rainforests (3-70 years) have shown that the basal area, biomass, maximum height and stem diameter at breast height have a negative and weak linear correlation with the reflectance data obtained by the Landsat 5 satellite sensors in the visible (blue, green and red) and infrared regions (Vieira et al. 2003, Ponzoni & Rezende 2004). Visible reflectance (Landsat data) is poorly predictive when forest biomass is over 150 t/ha, corresponding to 15 years of succession in tropical rainforests (Steininger 2000). Vegetation indices such as the Normalized Difference Vegetation Index (NDVI) and the SAVI (Soil Adjusted Vegetation Index) have also shown weak correlations with vegetation structure descriptors in chronosequences of Amazon rainforests (Vieira et al. 2003). Even data from a high spatial resolution sensor, Clark et al. (2004) identified significant and moderate correlations with basal area, height and biomass in chronosequences of tropical rainforest in Costa Rica. Part of these limitations seem to

have a fundamental cause inherent to optical remote sensing: the sensor fails to capture the structural variations under a closed canopy, typical of rainforests (Franklin 2001).

Succession studies combining remote sensing data and field-measured attributes of plant communities in dry regions are scarce and have shown contradictory results. Analyzes carried out in dry forests in Costa Rica, Mexico, and Venezuela have demonstrated significant relationships between remote sensing data (Landsat, Quickbird, LiDAR) and vegetation attributes over succession (Feeley et al. 2005, Castillo et al. 2012, Gallardo-Cruz et al. 2012). On the other hand, it has already been demonstrated that spectral indices, such as NDVI (ETM+ sensor/Landsat 7), present similar values in intermediate and late stages (Arroyo-Mora et al. 2005), being little predictive. In non-forest physiognomies, the few existing studies have shown that near-infrared reflectance and the NDVI index (Landsat satellite) are sensitive to variations in species richness and tree canopy cover (Yang et al. 2012, Medeiros et al. 2019). The lack of information and the inherent limitations of remote sensing reinforce the need to carry out further studies in dry regions and identify the potential of remotely-sensed data in characterizing the succession of plant communities.

In general, vegetation reflectance is based on differences in illumination, absorption and shading, which are related to tree top dimensions and spacing, photosynthetic and non-photosynthetic components, soil and lighting geometry (Franklin 2001, Asner 2004). Considering the vegetation, leaves constitute the main interaction element with electromagnetic radiation. Due to the mesophyll structure and photosynthetic pigments, leaves absorb especially in blue and red wavelengths and reflect mainly in the green and near-infrared

wavelengths of the electromagnetic spectrum (Willstätter & Stoll 1918). In the dry season, due to the degradation of photosynthetic pigments, vegetation spectral curves do not show absorption in the blue and red wavelengths (Asner 2004, Hörtensteiner 2006, Morais et al. 2021).

In addition to leaf interaction, characteristics such as density and distribution of individuals, AGB, shade fraction variations and phenology interfere with the spectral response of vegetation (Asner & Warner 2003, Galvão et al. 2015). In dry climate regions, where most plants shed their leaves in response to periods of water stress, non-photosynthetic components (aboveground dead-standing biomass and soil litter layer) constitute an essential proportion of the vegetation and contribute significantly to the canopy reflectance (Asner 2004). Studies in the Caatinga (thorny woodland in northeastern Brazil) have demonstrated that the litter carbon stock increases as succession progresses and that the leaves constitute the main component in all successional stages (Moura et al. 2016). Hence, it is likely that the non-photosynthetic components of the vegetation are a determining factor in the spectral characterization of successional stages of the Caatinga, especially during the dry season.

The choice of the sensor configures an a critical aspect of vegetation characterization. Remote sensing technology encompasses a variety of passive sensors ranging from multispectral sensors (Landsat, SPOT, RapidEye, etc.) to hyperspectral (Hyperion satellite) and active (LiDAR) sensors (Sánchez-Azofeifa et al. 2017). Given this variety, selecting a data source appropriate to the study area and identifying its limitations and advantages is essential. LiDAR data, for example, can distinguish among species in particular cases based on tree architecture (Sánchez-Azofeifa et al. 2017). However, like

hyperspectral sensors, it is not available for free, which limits its use. On the other hand, data from the Landsat mission has a broad historical series, global coverage, and free access. Analyses in semi-arid woodlands in Brazil and the United States have shown that Landsat data accurately estimate crown cover and plant species richness (Yang et al. 2012, Medeiros et al. 2019).

The vegetation of the Caatinga presents a non-forest physiognomy (in most of its extension), a predominance of deciduous species, an ephemeral herbaceous stratum and a discontinuous canopy (Queiroz et al. 2017). Due to itinerant agricultural practices and livestock, the Caatinga is quite fragmented and is under strong anthropic pressure (Leal et al. 2005, Sampaio 2010, Antongiovanni et al. 2018). Estimates based on remote sensing techniques on the percentage of natural vegetation cover indicate contradictory results. According to Beuchle et al. (2015), about 63% of the natural vegetation remains in the region. On the other hand, Silva & Barbosa (2017) suggest that at least 63.3% of the vegetation is under anthropogenic influence. A better understanding of the relationship between remotely-sensed data and attributes of the Caatinga plant community over succession can improve future vegetation cover modeling and produce more realistic estimates.

In this study, we characterize the spectral behavior of fragments of caatinga vegetation with different recovery ages and investigate whether Landsat data (reflectance and vegetation indices) can reflect the changes that occur in the vegetation structure along the succession. Whereas the energy reflected by the canopy and recorded by remote sensors is influenced by several factors, including those intrinsic to the image, and the Caatinga vegetation is subject to a seasonal climate, we decided to evaluate the spectral behavior of the fragments at the end

of the rainy season and during the dry season, according to the availability of images.

MATERIALS AND METHODS

Study site

We realized this study in the Caatinga Phytogeographical Domain (Andrade-Lima 1981, Araújo et al. 2005), or Caatinga Domain, located between 3° and 8° South latitude in northeastern Brazil. In most of the Caatinga Domain, the rainy season lasts between three and five months, rains are irregular, annual mean total rainfall is less than 750 mm (Andrade-Lima 1981, Araújo et al. 2005), and potential evapotranspiration can reach more than double the rainfall due to high temperatures, around 27°C (Nimer 1989). The physiognomy of the vegetation varies greatly and is related to variations in rainfall, soil and relief (Moro et al. 2015, 2016). Based on Holdridge's Life Zones (Holdridge 1967), the Caatinga encompasses a mosaic of Tropical Very Dry Forest and Thorn Woodland at altitudes below 500-600 m and Dry Forest at higher altitudes. In this study, the community can be classified as Thorn Woodland.

The caatinga is predominantly composed of non-forest physiognomies with two distinct strata. The woody stratum comprises deciduous and often thorny shrubs, trees and arborescent terrestrial cactus. The herbaceous stratum vegetates only during the rainy season and mainly contains broad-leaved terophytes and grasses (Carvalho et al. 2007, Mamede & Araújo 2008). In this stratum, there are also subshrub cacti and bromeliads with spikes.

The caatinga vegetation has been influenced by human activities since before European colonization when it was used by indigenous peoples as a hunting territory and for fruit collection and agriculture (Araújo Filho & Carvalho 1997). From the eighteenth century,

there was expansion of cattle ranching and cotton cultivation (Andrade 1979), and it is currently deforested for agropastoral activities and extraction of wood for energy (Araújo & Silva 2010). Deforested areas are generally used for a period of two consecutive years (Araújo Filho & Carvalho 1997) and then abandoned for four to 25 years (Brasil 2009, Riegelhaupt et al. 2010a, b). Therefore, the caatinga cover currently consists of a mosaic of fragments in different stages of recovery (Sampaio 2010). In a recent analysis, Antongiovanni et al. (2018) identified that the Caatinga is quite fragmented and susceptible to anthropic pressure. The same authors observed that 74% of the vegetation fragments have an area smaller than 50 ha.

For this study, we selected fragments with different recovery ages in and around the Aiuaba Ecological Station (ESEC) (40° 8' 6.564" W - 6° 37' 4.475" S, Fig. 1), municipality of Aiuaba, State of Ceará, northeastern Brazil. Koeppen classifies the climate as semi-arid BSh (Alvares et al. 2013), and has an average annual temperature of 25°C, average total annual rainfall of 580 mm (with rainfall concentrated between January and May), and potential evapotranspiration of 1397 mm per year, according to the FUNCEME database (<http://www.funceme.br>) for the period from 1985 to 2016) (Fig. 2).

Selection of vegetation fragments

To determine the age of each fragment, we used satellite images taken by the Landsat program between 1985 and 2014, and an aerial photograph taken in 1963, which was obtained from the Brazilian Geological Service (CPRM), USGS-NASA (<http://earthexplorer.usgs.gov/>) and INPE (<http://www.dgi.inpe.br/CDSR/>). Before analyzing the images, we applied a geometric correction using the "registration" module of the program ENVI 5.0 (RMS error <1) (Harris Geospatial Solutions, Inc.). We selected 12 fragments, which

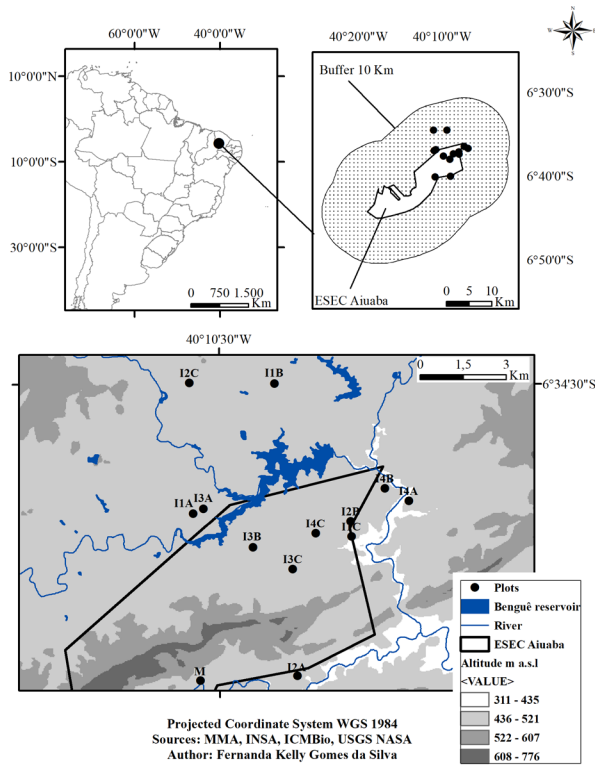


Figure 1. Location of the fragments analyzed in the chronosequence: I1 (10-15 years), I2 (20-25 years), I3 (30-35 years), I4 (40-45 years) and M (reference vegetation). A, B and C indicate the replications.

we called “communities in recovery”, distributed in four age intervals: **I1** (10-15 years), **I2** (20-25 years), **I3** (30-35 years) and **I4** (40-45 years) (Fig. 1). For each of these intervals, three replicates were delimited. We also selected a fragment with more than 52 years of recovery as a reference of mature vegetation or advanced succession (M) (Fig. 1), totaling 13 analyzed fragments. Each selected fragment had an average area of 7.3 ha (standard deviation \pm 4.5) and a minimum distance of 1 km, distributed over similar altitudes, varying from 443 to 510 m a.s.l. (Fig. 1). The soils of the studied communities were classified as Leptosols, Regosols and Cambisols (FAO nomenclature). They are shallow, with a predominance of loamy, sandy texture in the 0-20 cm surface layer and have high levels of assimilable phosphorus (P), organic matter

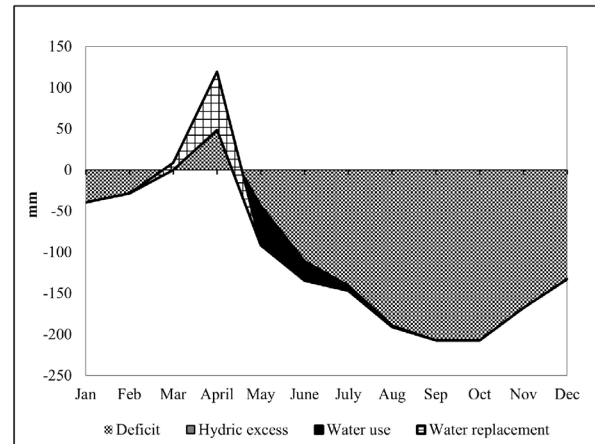


Figure 2. Climatological water balance (FAO/ Penman-Monteith’s method), municipality of Aiuaba (40°28’6.564” W/ 6°37’4.475” S), State of Ceará, northeastern Brazil. Monthly data of average, maximum and minimum temperature, rainfall, relative humidity (%), insolation and wind speed from 1985 to 2016, made available by Ceará State Foundation for Meteorology and Water Resources (FUNCEME). Soil water capacity = 100 mm. Diagram and calculations performed on the bHídrico GD 4.0 spreadsheet (D’Angiolella & Vasconcellos 2004).

(OM) and total organic carbon (TOC). Regarding composition, *Cenostigma bracteosum* (Tul.) Gagnon & G.P. Lewis, *Croton blanchetianus* Baill. and *Mimosa tenuiflora* (Willd.) Poir. were the most abundant species. The evergreen species (*Cynophalla flexuosa* (L.) J. Presl and *Ziziphus joazeiro* Mart.) were more abundant or exclusive in M.

Vegetation data collection

During the rainy season (March to April) of 2015, we delimited a plot of 0.1 hectare (Castanho et al. 2020) in the center of each fragment and recorded its geographical coordinates (plot vertices) with a Trimble Juno SC GPS (1m accuracy). In each plot, we sampled all trees with stem circumference at the ground level (PGL) \geq 9.4 cm, following Rodal et al. (2013), and we measured the PGL and the height of each tree. Based on the data collected in each plot, we calculated the total density (TD, number

of stems/ha), mean height (H, in m) and total basal area (G, in m²/ha) through the Mata Nativa software (Cientec 2006). We also calculated the aboveground biomass (AGB, in t/ha) from the diameter at ground level (DGL) using the equation $AGB = 0.0644 * DGL^{2.3948}$ (Sampaio & Silva 2005), in which $DGL = PGL / \pi$. Table I describes the structural differences between the analyzed age intervals.

Remote sensing data

We used images from the Landsat 8-9, Collection 2 platform, available at the surface reflectance level, with a temporal resolution of 16 days. Landsat 8-9 OLI surface reflectance products are generated using the Land Surface Reflectance Code (LaSRC) algorithm and are obtained free of charge from <https://earthexplorer.usgs.gov/>. We searched for images referring to the

Table I. Structure attributes of Caatinga woody plant communities with different recovery ages, Aiuaba Ecological Station, municipality of Aiuaba, State of Ceará, Brazil. H: Mean height (in m), G: Total basal area (in m²/ha), TD: Total density (number of stems/ha), AGB: Above ground biomass (in t/ha).

Age intervals	Fragments	H	G	TD	AGB
10-15 years	I1A	2,51	2,48	430,00	5,38
	I1B	3,43	5,84	670,00	13,04
	I1C	2,73	3,86	400,00	8,96
	Median	2,73	3,86	430,00	8,96
	Interquartile-Range	0,46	1,68	135,00	3,83
20-25 years	I2A	4,41	21,86	3760	44,09
	I2B	3,98	16,61	5920	31,18
	I2C	5,59	15,82	2120	34,12
	Median	4,41	16,61	3760,00	34,12
	Interquartile-Range	0,81	3,02	1900,00	6,46
30-35 years	I3A	4,97	17,5	2470	38,81
	I3B	3,66	20,13	3430	44,02
	I3C	4,19	21,8	2950	49,32
	Median	4,19	20,13	2950,00	44,02
	Interquartile-Range	0,66	2,15	480,00	5,25
40-45 years	I4A	4,71	16,69	2900	35,13
	I4B	5,19	15,46	3240	30,15
	I4C	4,04	19,62	3390	43,61
	Median	4,71	16,69	3240,00	35,13
	Interquartile-Range	0,58	2,08	245,00	6,73
> 52 years	M	5,64	41,17	3170	112,68

year 2015 (vegetation sampling). We found four images with low cloud cover: 07/07/2015 (end of the rainy season), 08/08/2015, 08/24/2015 and 09/25/ 2015 (dry season), which reinforces the difficulty of finding scenes with low cloud cover during the rainy season (see Mas et al. 2021).

We used bands from the visible region (blue, green and red), NIR and medium infrared (SWIR 1 and 2), which have a spatial resolution of 30 m, and we calculated two vegetation indices: NDVI (normalized difference vegetation index) and SAVI (soil-adjusted vegetation index) according to equations 1 and 2. We prioritized remote sensing products that are widely used, including in Caatinga, and that present less calculation and processing complexity (Morais et al. 2021).

$$\text{NDVI} = (\text{NIR} - \text{Red}) / (\text{NIR} + \text{Red}) \quad (\text{Equation 1})$$

$$\text{SAVI} = (1+L)(\text{NIR} - \text{Red}) / (L + \text{NIR} + \text{Red}) \quad (\text{Equation 2})$$

Where: L=0.5; NIR: surface reflectance in near-infrared band; Red: surface reflectance in the red band.

For each image, we extracted the mean surface reflectance and vegetation index values based on the polygon of the plot using the “Zonal Statistics” tool of the Quantum GIS 2.18 software (QGIS 2018). The polygons were constructed based on the geographical coordinates (plot vertices) taken from the phytosociological sampling. All remotely-sensed data (reflectance data and NDVI/SAVI indices) are available in Supplementary Material - Table S1.

To characterize the spectral behavior of vegetation at different recovery ages, we plot the mean values of surface reflectance (blue, green, red, near-infrared and short-wave infrared) for each plot and for each date in graphs called spectral reflectance curves. Additionally, we selected plots at different ages in a two-dimensional space of attributes (scatter diagram),

in which each pixel is located as a point whose coordinates are given by its reflectance values in the red and near-infrared band. This approach is analogous to the Greenness and Brightness concept formulated by Kauth & Thomas (1976). It is understood that each element of the scene (water, vegetation, soil, etc.) occurs in different proportions within the same pixel, and those pixels that have the “purest” proportions are located at the extremes of the two-dimensional distribution, which assumes a form triangle or gnomon hat (Ponzoni et al. 2012). In the lower-left portion are the pixels related to bodies of water and shaded regions. The pixels that represent the exposed soils are located in the right vertex, with average reflectance values. And in the upper left vertex are located the pixels occupied by the proportions of vegetation cover (Ponzoni et al. 2012). We used the 2D scatter plots tool in the ENVI 5.0 program.

Data analysis

We tested the normality of all variables using the Shapiro-Wilk test ($p > 0.05$). To investigate the existence of a relationship between the structure attributes (total density, mean height, total basal area and aboveground biomass) and the remotely-sensed data (reflectance data in blue, green, red, near-infrared and short-wave infrared and NDVI/SAVI indices), we applied Spearman correlation analyses, considering the level of significance of $p < 0.05$. We used Spearman analyses because we found non-normal data (total basal area, reflectance in the green, red and near-infrared regions, and SAVI and NDVI indices). We used the data obtained for each community/plot. All analyzes were performed in the R program (R Core Team 2022).

RESULTS

Spectral behavior of Caatinga fragments with different recovery ages

We observed (Fig. 3), except for the near-infrared (NIR), that the reflectance values of the analyzed bands are higher in communities between 10 and 15 years old (I1), intermediate and overlapping in communities I2, I3 and I4 and lower in the community aged over 52 years (M). For NIR reflectance, the values found for I2, I3, I4 and M were too close in the images obtained on August 8th, August 24th and September 25th, 2015. In the image taken on July 7th, we observed that the NIR reflectance referring to mature vegetation was higher than the NIR of the other communities.

A fact that drew attention refers to the spectral curve of mature vegetation in the image of July 7, 2015, with characteristics of photosynthetically active vegetation, showing absorption in the blue and red bands, greater reflectance in the green and NIR bands, and again short-wave infrared absorption. In the subsequent images, we observe that the spectral curve of the mature community is similar to the curves of the other communities, with increasing reflectance from blue to NIR and absorption in the short-wave infrared.

By selecting vegetation fragments with different ages in the two-dimensional pixel space (Fig. 4a-b), we identified that some communities are located in different regions of the graph. Communities aged between 10 and 15 years (I1) are represented by pixels located on the right vertex or closer to it, which denotes a greater representation of exposed soil in these areas. Except for the July/2015 image, the I1 fragments have the highest reflectance values in the red and near-infrared regions. Communities aged between 20 and 45 years old, which comprise intervals I2, I3 and I4, have an overlap of pixels

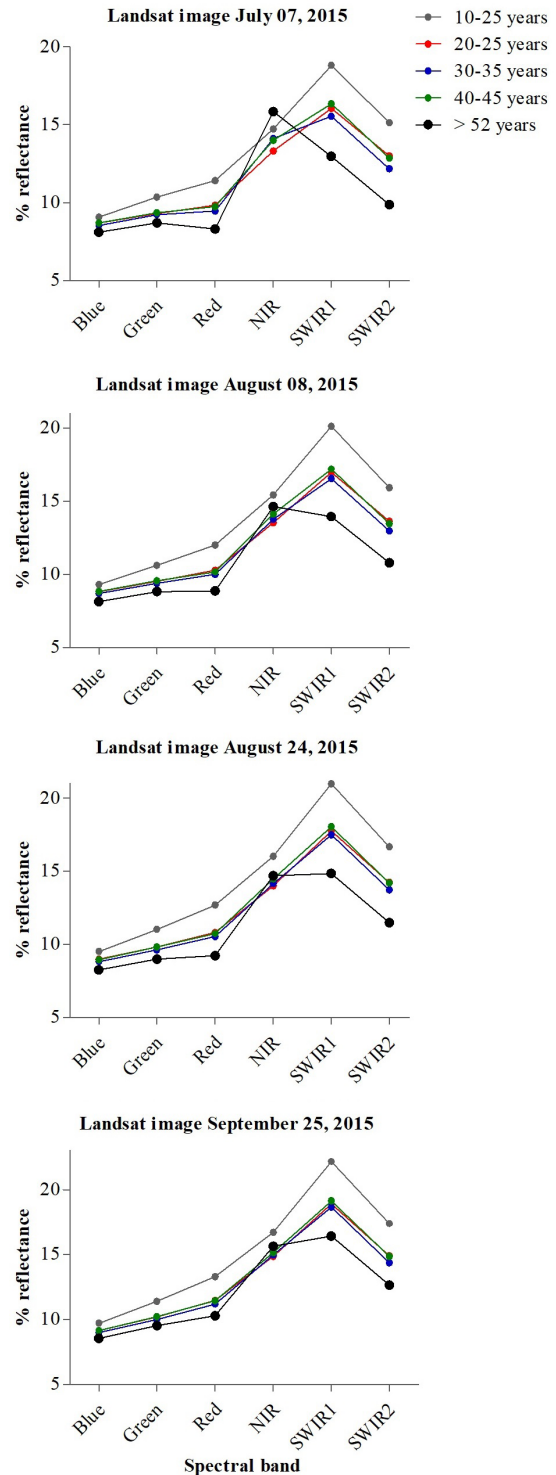


Figure 3. Spectral curves of Caatinga vegetation fragments with different recovery ages at the end of the rainy season (July 07, 2015) and during the dry season (August 08, 2015; August 24, 2015; September 25, 2015), Aiuaba Ecological Station, municipality of Aiuaba, State of Ceará, Brazil.

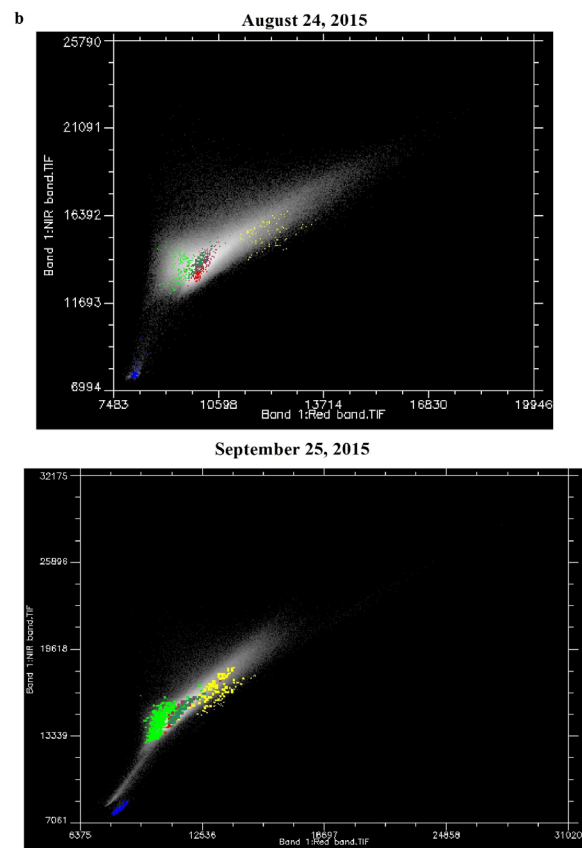
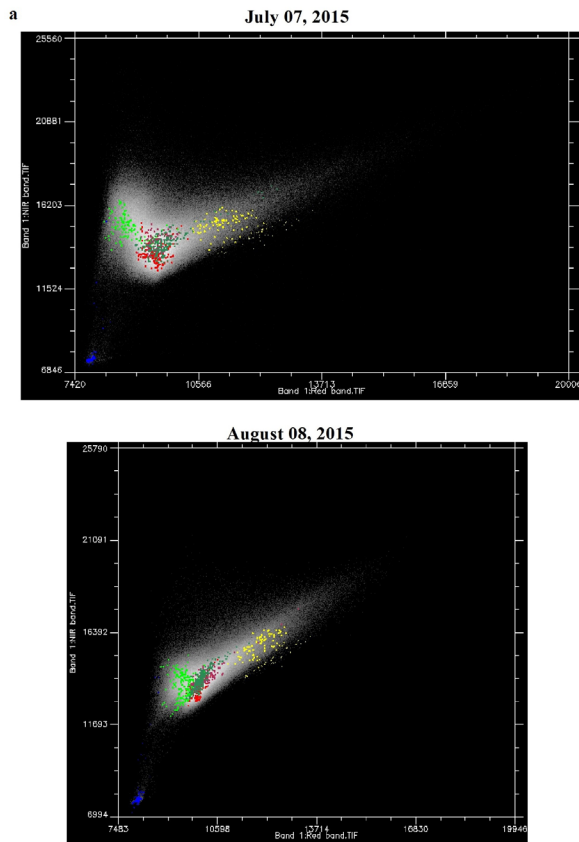


Figure 4a. Scatter plots with surface reflectance data Red (x-axis) - NIR (y-axis) of the Caatinga with different recovery ages (July 07, 2015; August 08, 2015). The pixels are represented with the following colors: Yellow for communities aged 10-15 years, Red for communities aged 20-25 years, Maroon for communities aged 30-35 years, Sea green for communities aged 40-45 years, Green for the community with a minimum age of 52 years (M) and Blue for water (Benguê Reservoir, as shown in Fig. 1).

Figure 4b. Scatter plots with surface reflectance data Red (x-axis) - NIR (y-axis) of the Caatinga with different recovery ages (August 24, 2015; September 25, 2015). The pixels are represented with the following colors: Yellow for communities aged 10-15 years, Red for communities aged 20-25 years, Maroon for communities aged 30-35 years, Sea green for communities aged 40-45 years, Green for the community with a minimum age of 52 years (M) and Blue for water (Benguê Reservoir, as shown in Fig. 1).

in two-dimensional space, which means that the analyzed time interval did not reflect on spectral differences in the red and near-infrared bands. In addition, the pixels are in an intermediate region, which may constitute a space of greater spectral mixing, compared to the other areas. Regarding the mature community (M), we observed that the pixels are projected to the left, representing lower values in red reflectance and a more significant influence of the shading factor and/or vegetation.

Here, it is essential to highlight the arrangement of the “cloud” of mature vegetation pixels (M) in the July/2015 image (Fig. 4a). In this scene (and as observed in the spectral curves), the most conserved vegetation presents a typical spectral response of photosynthetically active vegetation, with high values in the near-infrared region and lower values in the red region. In the July/2015 image, it is also clear that the “clouds” of pixels referring to communities aged 10-15 (I1), 20-45 (I2, I3, I4) and 52(M) years old are located

in better-defined spaces, that is, with a smaller pixel overlap.

Relationship between woody vegetation attributes and remotely-sensed data along succession

Considering the July 2015 image, we observed that, among the significant correlations of interest ($p < 0.05$), about 53% were strong ($\rho \geq 0.7$) and 47% moderate, with $\rho = 0.6$ (Fig. 5a).

Reflectance data in the blue, red and short-wave infrared region (SWIR 1 and 2) were negatively correlated with mean height (H), basal area (G) and biomass (AGB). The correlation coefficient between these variables ranged from -0.63 to -0.79, indicating that as H, G and AGB increase, reflectance decreases (Fig. 5a). The NDVI and SAVI indices were positively correlated with G and AGB, with coefficients between 0.67 and 0.78.

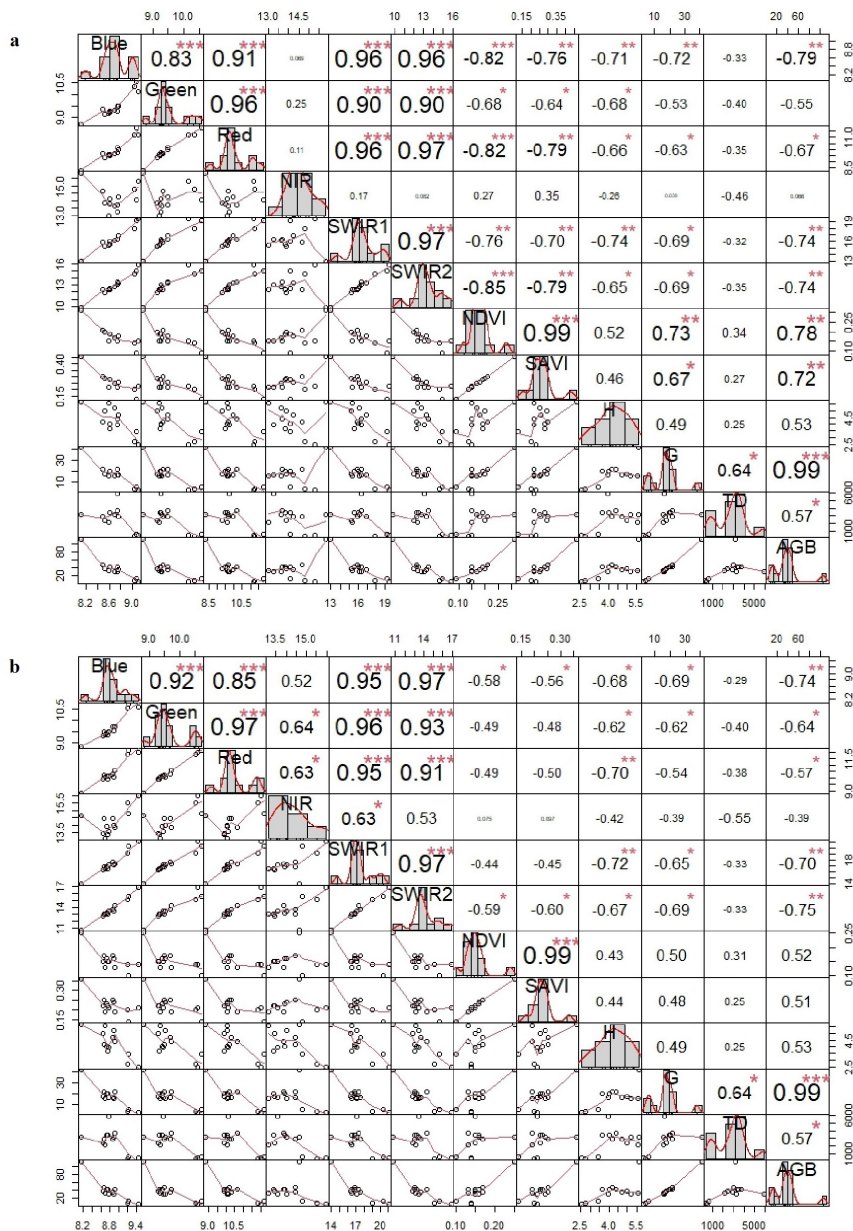


Figure 5. Spearman correlations between Caatinga vegetation structure attributes and remotely-sensed data obtained from Landsat 8 images on July 7, 2015 (a) and August 8, 2015 (b). The distribution of each variable is observed diagonally. At the bottom of the diagonal the bivariate scatterplots with a fitted line are displayed. At the top of the diagonal, the correlation value and the significance level with stars are displayed, where the p-value is equal to 0.001***, 0.01** and 0.05*. H: Mean height (in m), G: Total basal area (in m²/ha), TD: Total density (number of stems/ha), AGB: Above ground biomass (in t/ha).

Considering the August 8 image, we found that, among the significant correlations of interest ($p < 0.05$), about 36% were strong ($p \geq 0.7$) and 64% moderate, with p between 0.5 and 0.6 (Fig. 5b). Reflectance data in the blue, green and short-wave infrared bands (SWIR 1 and 2) were negatively correlated with H, G and AGB. Contrary to what was observed in the July scene, no attribute was related to the SAVI and NDVI indices.

In the August 24th image (Fig. 6a), we observed that all visible and short-wave infrared bands correlated negatively with H, G and AGB, with coefficients between -0.56 and -0.75. With regard to indices, only SAVI was sensitive to increases in G and AGB ($\rho_{SAVI/G} = 0.59$; $\rho_{SAVI/AGB} = 0.62$). Among the significant correlations ($p < 0.05$), about 24 and 76% were strong and moderate, respectively.

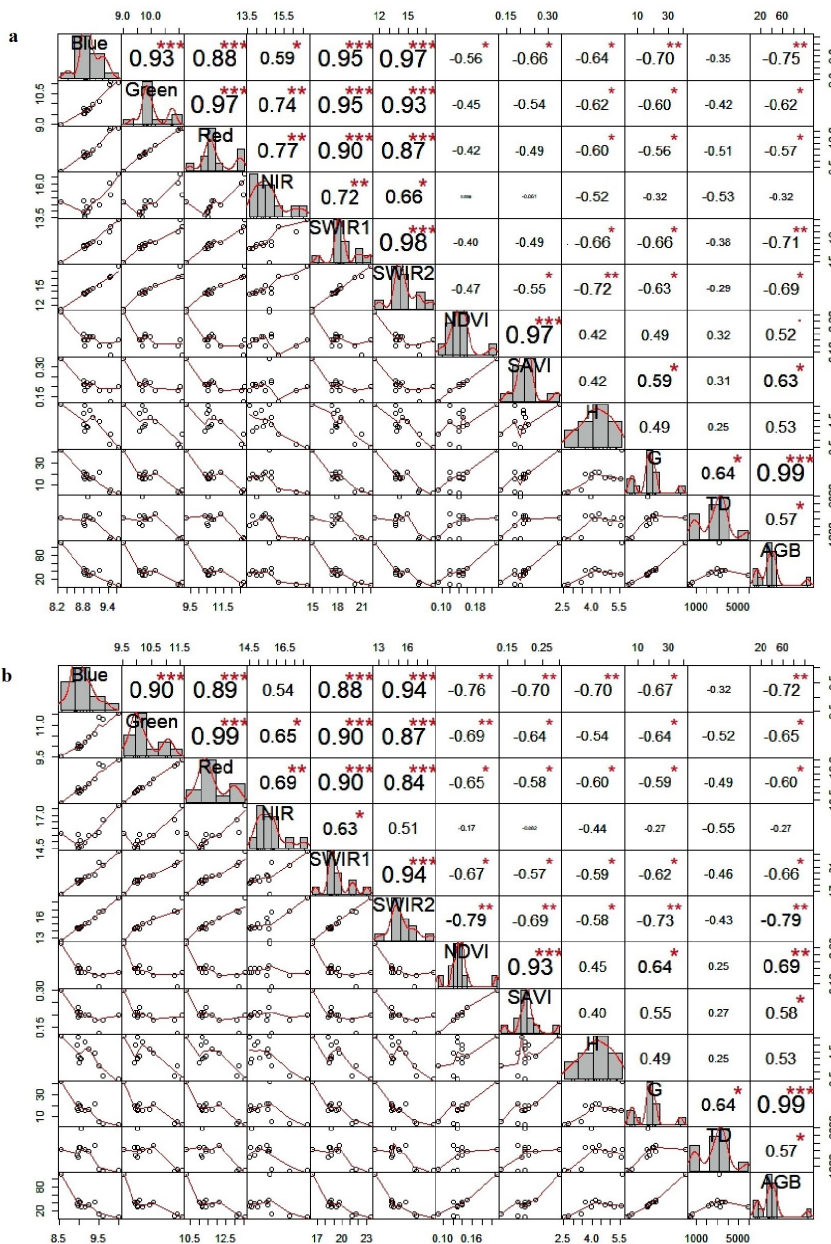


Figure 6. Spearman correlations between Caatinga vegetation structure attributes and Landsat 8 remotely-sensed data obtained on August 24, 2015 (a) and September 25, 2015 (b). The distribution of each variable is observed diagonally. At the bottom of the diagonal the bivariate scatterplots with a fitted line are displayed. At the top of the diagonal, the correlation value and the significance level with stars are displayed, where the p-value is equal to 0.001*, 0.01** and 0.05*.** H: Mean height (in m), G: Total basal area (in m²/ha), TD: Total density (number of stems/ha), AGB: Above ground biomass (in t/ha).

Finally, when analyzing the image obtained on September 25th (Fig. 6b), we identified that the relationship between the attributes H, G and AGB and reflectance in the visible region and SWIR 1 and 2 was similar to those previously found, with coefficients between -0.58 and -0.79. NDVI was sensitive to variation in G and AGB ($\rho_{\text{NDVI/G}} = 0.64$; $\rho_{\text{NDVI/AGB}} = 0.69$), while SAVI responded positively only to variation in total aboveground biomass ($\rho_{\text{SAVI/AGB}} = 0.58$).

In summary, we identified that the relationship between blue and short-wave infrared reflectance and the H, G and AGB attributes was maintained in the four analyzed images. As H, G and AGB increase, reflectance decreases in these spectral bands (Fig. 5, Fig. 6). On the other hand, we observed that the near-infrared reflectance data did not correlate with the analyzed structural attributes and that the response of the vegetation indices oscillated between the analyzed dates. Another factor that drew attention was the decrease in the correlation coefficients over the dates, indicating that the significant correlations tend to be predominantly strong when we analyze images from the end of the rainy season and largely moderate when we analyze images at the peak of the dry season.

DISCUSSION

Our results indicate that successional changes in non-forest physiognomies, such as the Caatinga, are perceived from Landsat data. The energy reflected by the canopy and recorded by remote sensors is interfered with by several factors, including vegetation characteristics (phenology, physiognomy, structure, species composition), sensor (spatial, radiometric, and spectral resolution, for example) and geometric and sight factors (Franklin 2001, Ponzoni & Rezende 2004, Ponzoni et al. 2012, Barbosa

et al. 2014). Considering that the Caatinga vegetation predominantly presents an open and discontinuous canopy, our results reinforce the understanding that the amount of vegetation viewed from above interferes with the detection of community features. According to Franklin (2001), if the canopy is open, the reflectance can be correlated with other attributes, such as understory characteristics which may be indirectly related to the target variables; if the canopy is closed, the extent to which other parameters can be predicted seems to depend on the extent to which a closed canopy can predict them. In rainforests, which accumulate more than 200 t/ha of aboveground biomass in mature communities (Vieira et al. 2003, Galvão et al. 2015) and have a closed canopy, authors have observed weak correlations between the structural descriptors and the reflectance data obtained from remote sensing. Even using reflectance data, such as blue (0.45-0.52 μm), green (0.51-0.60 μm), red (0.63-0.70 μm), and near-infrared (0.76-0.85 μm) obtained from a high spatial resolution sensor (1 and 4m), Clark et al. (2004) found few moderate and significant correlations in forests in Costa Rica: between 8 and 11% among 84 and 264 possible, respectively. Visible reflectance (Landsat data) is poorly predictive when forest biomass is over 150 t/ha, corresponding to 15 years of succession in tropical rainforests (Steininger 2000). On the other hand, studies carried out in non-forest physiognomies have demonstrated significant empirical relationships between structure attributes and reflectance data and NDVI/SAVI indices (Yang et al. 2012, Almeida et al. 2014).

It is possible to highlight two important aspects related to the spectral behavior of the communities along the succession: soil exposure and the non-photosynthetic component of the vegetation. Even by analyzing images from the dry period, it was possible to detect that

younger communities present, in their spectral response, the great influence of the exposed soil, evidenced by the high reflectance values (Franklin 2001) and by the disposition in the two-dimensional space of pixels. The high reflectance values of younger communities were evident in all bands and images, except for NIR in the July image. As succession progresses, the increase in basal area, biomass and individuals produces a shading effect and, consequently, a reduction in reflectance. Even in savannas, Asner & Warner (2003) demonstrated that the shade fraction is determinant in the spectral response of the vegetation. These authors found that as the total density of individuals increases in savannah communities, the shadow fraction also increases, accounting for up to 50% of the decrease in red band reflectance.

The spectral behavior of vegetation fragments (except for mature vegetation in the July 7th image) is strongly influenced by the non-photosynthetic component, represented by stems, branches and litter. In regions with a dry climate, this component plays a crucial role in the spectral signature of vegetation due to the loss of leaves by most plants during the dry season. Leaf senescence and the subsequent degradation of photosynthetic pigments inhibit or significantly reduce the absorption of electromagnetic energy in the blue and red region (Asner 2004, Hörtensteiner 2006), as demonstrated here and by Asner (2004) and Morais et al. (2021). On the other hand, the spectral behavior of the mature vegetation fragment (M) on July 7th represents a more significant influence of photosynthetically active vegetation (green leaves), with the absorption of energy in blue and red and high reflectance in near-infrared. This spectral behavior may result from the edaphic conditions of the M fragment. In a study carried out in dry forests in Minas Gerais, Brazil, Pezzini et al. (2014) observed

some marked differences in the timing of leaf phenology between early and more advanced successional stages. These authors identified that the percentage of individuals with green leaves is correlated with climatic (precipitation and relative humidity) and edaphic factors, such as soil water content. It is possible that the local conditions of the M fragment contribute to the delay in leaf senescence and, consequently, to the observed spectral response.

As the reflectance in the blue and short-wave infrared regions showed a significant correlation with the mean height, basal area and total biomass, regardless of the analyzed image, we suggest that these remotely-sensed data be prioritized in future analyzes of the Caatinga vegetation from Landsat images. The SWIR region (1-3 μm) is sensitive to the water content present in plants and soil due to the absorption of electromagnetic energy at this wavelength (Ji et al. 2011). SWIR reflectance generally decreased as water content increased (Ji et al. 2011). As we did not measure soil moisture data, we cannot state that the decrease in SWIR over the succession is directly related to soil characteristics. We speculate that this relationship is possible due to the increase in litter deposition over time, as demonstrated by Moura et al. (2016).

Considering that the correlations between the structural attributes and the remote sensing variables were predominantly strong right after the rainy season and that, throughout the dry period, there is degradation of the leaves recently lost by most plants, we recommend that analyzes of the Caatinga prioritize satellite images obtained just after the rainy season. In this way, it is possible to acquire scenes with low cloud cover and a better representation of the non-photosynthetic component of the vegetation. The arrangement of the fragments in the two-dimensional pixel space showed a better separation of the communities aged

10 to 15 years, 20 to 45 years and 52 years, corroborating this suggestion.

CONCLUSION

This study demonstrates that Landsat image data can characterize the conservation status of non-forest physiognomies, such as the Caatinga. The spectral differences observed between fragments aged 10-15 years, 20-45 years and >52 years correspond to changes in vegetation structure over the succession, specifically in the mean height of individuals, basal area and total biomass aboveground. Our results suggest that reflectance in the blue and short-wave infrared regions should be prioritized in future band compositions and modeling.

Judging from the spectral variation of the analysed chronosequence and the Caatinga deciduousness in the dry season, we conclude that the litter layer (a non-photosynthetic vegetation component) and the soil exposure influence the spectral data. We hope our results can subsidize future studies mapping different successional stages of the crystalline Caatinga and other similar vegetation types.

Acknowledgments

This study was financed in part by the Coordenação de Aperfeiçoamento de Pessoal de Nível Superior- Brazil (CAPES)- Finance Code 001. We also thank Conselho Nacional de Desenvolvimento Científico e Tecnológico (CNPq) for research grants to F. R. Martins and F. S. Araújo and financial support (process 620045/2008-6); CNPq/ICMBio for financial support (process 551998/20113); INCT IN-TREE: Inter-disciplinary and transdisciplinary studies in ecology and evolution (CNPq CAPES/FAPESB); to the managers of the Aiuaba Ecological Station for logistical support; PhD Ellen Cristina Dantas de Carvalho and Marcelo Boccia Leite for assistance in the collection of field data; Instituto Chico Mendes de Conservação da Biodiversidade (ICMBio) for authorizing data collection in the study area (#47639).

REFERENCES

- ALMEIDA AQ, MELLO AA, DÓRIA NETO AL & FERRAZ RC. 2014. Relações empíricas entre características dendrométricas da Caatinga brasileira e dados TM Landsat 5. *Pesq Agropec Bras* 49(4): 306-315.
- ALVARES CA, STAPE JL, SENTELHAS PC, DE MORAES GONÇALVES JL & SPAROVEK G. 2013. Köppen's climate classification map for Brazil. *Meteorol Zeitschrift* 22(6): 711-728.
- ANDRADE MC. 1979. O Processo de Ocupação do Espaço Regional do Nordeste, 2nd ed., Recife: SUDENE, 142 p.
- ANDRADE-LIMA D. 1981. The caatingas dominium. *Rev Bras Bot* 4(2): 149-163.
- ANTONGIOVANNI M, VENTICINQUE EM & FONSECA CR. 2018. Fragmentation patterns of the Caatinga drylands. *Landscape Ecol* (33): 1353-1367.
- ARAÚJO FILHO JA & CARVALHO FC. 1997. Desenvolvimento Sustentado da Caatinga, Sobral: EMBRAPA-CNPC, 19 p.
- ARAÚJO FS, RODALMUN & BARBOSA MRV. 2005. BIODIVERSIDADE DO BIOMA CAATINGA: Suporte a estratégias regionais de conservação, Brasília: Ministério do Meio Ambiente, 446 p.
- ARAÚJO LVC & SILVA JA. 2010. UNIDADE EXPERIMENTAL ASSENTAMENTO VENÂNCIO ZACARIAS-MACAU/RN. In: GARIGLIO MA, SAMPAIO EVSB, CESTARO LA & KAGEYAMA PY. *Uso Sustentável e Conservação dos Recursos Florestais da CAATINGA*, Brasília: Serviço Florestal Brasileiro, p. 245-255.
- ARROYO-MORA JP, SÁNCHEZ-AZOFEIFA GA, KALACSKA MER & RIVARD B. 2005. Secondary Forest Detection in a Neotropical Dry Forest Landscape Using Landsat 7. *Biotropica* 37(4): 497-507.
- ASNER GP. 2004. Biophysical remote sensing signatures of arid and semiarid ecosystems. In: USTIN SL (Ed), *Remote Sensing for Natural Resources Management and Environmental Monitoring: Manual of Remote Sensing*, New York: J Wiley & Sons, New York, USA, p. 53-109.
- ASNER GP & WARNER AS. 2003. Canopy shadow in IKONOS satellite observations of tropical forests and savannas. *Remote Sens Environ* 87(4): 521-533.
- BARBOSA JM, BROADBENT EN & BITENCOURT MD. 2014. Remote Sensing of Aboveground Biomass in Tropical Secondary Forests: A Review. *Int J For Res* 2014: ID715796.
- BEUCHLE R, GRECCHI RC, SHIMABUKURO YE, SELIGER R, EVA HD, SANO E & ACHARD F. 2015. Land cover changes in the Brazilian Cerrado and Caatinga biomes from 1990 to 2010 based on a systematic remote sensing sampling approach. *Appl Geogr* 58: 116-127.

- BRASIL. 2009. Instrução Normativa n.1 de 25 de Junho de 2009: Dispõe sobre procedimentos técnicos para elaboração, apresentação, execução e avaliação técnica de Planos de Manejo Florestal Sustentável-PMFS da Caatinga e suas formações sucessoras, e dá outras providências, Brasília: Ministério do Meio Ambiente.
- CARVALHO RC, ARAÚJO FS & LIMA-VERDE W. 2007. Flora and life-form spectrum in an area of deciduous thorn woodland (caatinga) in northeastern, Brazil. *J Arid Environ* 68: 237-247.
- CASTANHO ADA, COE M, ANDRADE EM, WALKER W, BACCINI A, CAMPOS DA & FARINA M. 2020. A close look at above ground biomass of a large and heterogeneous Seasonally Dry Tropical Forest-Caatinga in North East of Brazil. *An Acad Bras Cienc* 92: e20190282.
- CASTILLO M, RIVARD B, SÁNCHEZ-AZOFEIFA A, CALVO-ALVARADO J & DUBAYAH R. 2012. LIDAR remote sensing for secondary Tropical Dry Forest identification. *Remote Sens Environ* 121(2012): 132-143.
- CHAMBERS JQ, ASNER GP, MORTON DC, ANDERSON LO, SAATCHI SS, ESPÍRITO-SANTO FDB, PALACE M & SOUZA JR C. 2007. Regional ecosystem structure and function: ecological insights from remote sensing of tropical forests. *Trends Ecol Evol* 22(8): 414-423.
- CIENTEC. 2006. Mata Nativa 2: Sistema para a análise fitossociológica e elaboração de inventários e planos de manejo de florestas nativas, Viçosa: Grupo Cientec, 295 p.
- CLARK DB, READ JM, CLARK ML, CRUZ AM, DOTTE MF & CLARK DA. 2004. Application of 1-M and 4-M Resolution Satellite Data to Ecological Studies of Tropical Rain Forests. *Ecol Appl* 14(1): 61-74.
- CLEMENTS FE. 1916. *Plant Succession: An analysis of the development of vegetation*. Washington: Cornell University, 512 p.
- D'ANGIOLELLA G & VASCONCELLOS VLD. 2004. bHídrico GD 4.0-2004: planilha eletrônica para cálculo do balanço hídrico climatológico. *Bahia Agrícola* 6(3): 14-16.
- FEELEY KJ, GILLESPIE TW & TERBORGH JW. 2005. The Utility of Spectral Indices from Landsat ETM+ for Measuring the Structure and Composition of Tropical Dry Forests. *Biotropica* 37(4): 508-519.
- FAO - FOOD AND AGRICULTURE ORGANIZATION. 2010. *Global Forest Resources Assessment 2010 main report*, Rome: FAO For. Pap., 378 p.
- FRANKLIN SE. 2001. *Remote Sensing for Sustainable Forest Management*, Boca Raton: CRC Press, 424 p.
- GALLARDO-CRUZ JA, MEAVE JA, GONZÁLEZ EJ, LEBRIJA-TREJOS EE, ROMERO-ROMERO MA, PÉREZ-GARCIA EA, GALLARDO-CRUZ R, HERNÁNDEZ-STEFANONI JL & MARTORELL C. 2012. Predicting Tropical Dry Forest Successional Attributes from Space: Is the Key Hidden in Image Texture? *PLoS ONE* 7(2): 38-45.
- GALVÃO LS, ROBERTO J & AGNOL RD. 2015. Following a site-specific secondary succession in the Amazon using the Landsat CDR product and field inventory data. *Int J Remote Sens* 36 (2): 37-41.
- HOLDRIDGE LR. 1967. *Life zone ecology*, San Jose: Trop Sci, 206 p.
- HÖRTENSTEINER S. 2006. Chlorophyll Degradation During Senescence. *Annu Rev Plant Biol* 57(1): 55-77.
- JI L, ZHANG L, WYLIE BK & ROVER J. 2011. On the terminology of the spectral vegetation index (NIR-SWIR)/(NIR+SWIR). *Int J Remote Sens* 32(21): 6901-6909.
- KAUTH RJ & THOMAS GS. 1976. The tasseled Cap - A Graphic Description of the Spectral-Temporal Development of Agricultural Crops as Seen by LANDSAT. *Proceedings of the Symposium on Machine Processing of Remotely Sensed Data*, Indiana: Purdue University of West Lafayette, p. 4B-41 to 4B-51.
- LEAL IR, SILVA JMC, TABARELLI M & LACHER JR TE. 2005. Changing the Course of Biodiversity Conservation in the Caatinga of Northeastern Brazil. *Conserv Biol* 19(3): 701-706.
- LU D, MAUSEL P, BRONDÍZIO E & MORAN E. 2004. Relationships between forest stand parameters and Landsat TM spectral responses in the Brazilian Amazon Basin. *For Ecol Manag* 198(1-3): 149-167.
- LUCAS RM, HONZÁK M, CURRAN PJ, FOODY GM, MILNES R, BROWN T & AMARAL S. 2000. Mapping the regional extent of tropical forest regeneration stages in the Brazilian Legal Amazon using NOAA AVHRR data. *Int J Remote Sensing* 21(15): 2855-2881.
- MACKEY B ET AL. 2015. Policy Options for the World's Primary Forests in Multilateral Environmental Agreements. *Conserv Lett* 8: 139-147.
- MAMEDE MA & ARAÚJO FS. 2008. Effects of slash and burn practices on a soil seed bank of caatinga vegetation in Northeastern Brazil. *J Arid Environ* 72(4): 458-470.
- MARTINUZZI S, GOULD WA, VIERLING LA, HUDAK AT, NELSON RF & EVANS JS. 2012. Quantifying Tropical Dry Forest Type and Succession: Substantial Improvement with LiDAR. *Biotropica*, p. 1-12.
- MAS JF, SOPCHAKI CH, RABELO FDB, ARAÚJO FS & SOLORZANO JV. 2021. Análise da disponibilidade de imagens Landsat e Sentinel-2 para o Brasil. *Geog Ens Pesq* 24: e47.

- MAUSEL P, WU Y, LI Y, MORAN EF & BRONDIZIO ES. 1993. Spectral Identification of Successional Stages Following Deforestation in the Amazon. *Geocarto Int* 8(4): 61-71.
- MEDEIROS ESS, MACHADO CCC, GALVINCIO JD, MOURA MSB & ARAUJO HFP. 2019. Predicting plant species richness with satellite images in the largest dry forest nucleus in South America. *J Arid Environ* 166: 43-50.
- MORAIS LF, CAVALCANTE ACR, AQUINO DN, NOGUEIRA FHM & CÂNDIDO MJD. 2021. Spectral responses in rangelands and land cover change by livestock in regions of the Caatinga biome, Brazil. *Sci Rep* 11: 18261.
- MORO MF, NIC LUGHADHA E, DE ARAÚJO FS & MARTINS FR. 2016. A Phytogeographical Metaanalysis of the Semiarid Caatinga Domain in Brazil. *Bot Rev* 82(2): 91-148.
- MORO MF, SILVA IA, ARAÚJO FS, LUGHADHA EN, MEAGHER TR & MARTINS FR. 2015. The role of edaphic environment and climate in structuring phylogenetic pattern in seasonally dry tropical plant communities. *PLoS ONE* 10(3): 1-19.
- MOURA PM, ALTHOFF TD, OLIVEIRA RA, SOUTO JS, SOUTO PC, MENEZES RSC & SAMPAIO EVSB. 2016. Carbon and nutrient fluxes through litterfall at four succession stages of Caatinga dry forest in Northeastern Brazil. *Nutr Cycl Agroecosyst* 105: 25-38.
- NIMER E. 1989. *Climatologia do Brasil*. Rio de Janeiro: IBGE, 422 p.
- PAIN A, MARQUARDT K, LINDH A & HASSELQUIST NJ. 2021. What Is Secondary about Secondary Tropical Forest? Rethinking Forest Landscapes. *Human Ecology* 49: 239-247.
- PEZZINI FF, RANIERI BD, BRANDÃO DO, FERNANDES GW, QUESADA M, ESPÍRITO-SANTO MM & JACOBI CM. 2014. Changes in tree phenology along natural regeneration in a seasonally dry tropical forest. *Plant Biosystems - An International Journal Dealing with all Aspects of Plant Biology* 148(5): 965-974.
- PICKETT S, MEINERS SJ & CADENASSO ML. 2011. Domain and propositions of succession theory. In: SCHEINER SM & WILLIG MR (Eds.), *The theory of ecology*. The University of Chicago Press, Chicago and London, p. 185-226
- PONZONI FJ & REZENDE ACP. 2004. Caracterização espectral de estágios sucessionais de vegetação secundária arbórea em Altamira (PA), através de dados orbitais. *Rev Árvore* 28(4): 535-545.
- PONZONI FJ, SHIMABUKURO YE & KUPLICH TM. 2012. *Sensoriamento remoto da vegetação*, 2nd ed, São Paulo: Oficina de Textos, 176 p.
- QGIS DEVELOPMENT TEAM. 2018. QGIS Geographic Information System. Available from: <http://qgis.osgeo.org>.
- QUEIROZ LP, CARDOSO D, FERNANDES MF & MORO M. 2017. Diversity and evolution of flowering plants of the Caatinga domain. In: Silva JC, Leal I & Tabarelli M (Eds), *Caatinga: the Largest Tropical Dry Forest Region in South America*. Springer, Cham, p. 23-63.
- R CORE TEAM. 2022. R: A language and environment for statistical computing. R Foundation for Statistical Computing, Vienna, Austria. URL <https://www.R-project.org/>.
- RIEGELHAUPT E, PAREYN FGC & BACALINI P. 2010a. O Manejo Florestal na Caatinga: Resultados da Experimentação. In: GARIGLIO MA, SAMPAIO EVSB, CESTARO LA & KAGEYAMA PY. *Uso Sustentável e Conservação dos Recursos Florestais da CAATINGA*, Brasília: Serviço Florestal Brasileiro, p. 256-275.
- RIEGELHAUPT EM, PAREYN FGC & GARIGLIO MA. 2010b. O Manejo Florestal como Ferramenta para o Uso Sustentável e Conservação da Caatinga. In: GARIGLIO MA, SAMPAIO EVSB, CESTARO LA & KAGEYAMA PY. *Uso Sustentável e Conservação dos Recursos Florestais da CAATINGA*, Brasília: Serviço Florestal Brasileiro, p. 349-367.
- RODAL MJN, SAMPAIO EVSB & FIGUEIREDO MA. 2013. Manual sobre métodos de estudo florístico e fitossociológico: ecossistema caatinga, Brasília: Sociedade Botânica do Brasil, 37 p. <http://www.rstudio.com/>.
- SAMPAIO EVSB. 2010. CARACTERIZAÇÃO DO BIOMA CAATINGA. In: GARIGLIO MA, SAMPAIO EVSB, CESTARO LA & KAGEYAMA PY. *Uso Sustentável e Conservação dos Recursos Florestais da CAATINGA*, Brasília: Serviço Florestal Brasileiro, p. 29-48.
- SAMPAIO EVSB & SILVA GC. 2005. Biomass equations for Brazilian semiarid caatinga plants. *Acta Bot Brasilica* 19(4): 935-943.
- SÁNCHEZ-AZOFEIFA A, GUZMÁN JA, CAMPOS CA, CASTRO S, GARCIA-MILLAN V, NIGHTINGALE J & ANKINE C. 2017. Twenty-first remote sensing technologies are revolutionizing the study of tropical forests. *Biotropica*, p. 1-6.
- SILVA JMC & BARBOSA LCF. 2017. Impact of human activities on the Caatinga. In: SILVA JMC, LEAL I & TABARELLI M (Eds), *Caatinga: The Largest Tropical Dry Forest Region in South America*, Cham: Springer International Publishing, p. 359-368.
- SONG C, SCHROEDER TA & COHEN WB. 2007. Predicting temperate conifer forest successional stage distributions

with multitemporal Landsat Thematic Mapper imagery. *Remote Sens Environ* 106 (2): 228-237.

STEININGER MK. 2000. Satellite estimation of tropical secondary forest above-ground biomass: data from Brazil and Bolivia. *Int J Remote Sens* 21(6): 1139-1157.

TIMOTHY D, ONISIMO M, CLETAH S, ADELABU S & TSITSI B. 2016. Remote sensing of aboveground forest biomass: A review. *Trop Ecol* 57(2): 125-132.

VIEIRA G, SILVA A, ALMEIDA D, DAVIDSON EA & STONE TA. 2003. Classifying successional forests using Landsat spectral properties and ecological characteristics in eastern Amazônia. *Remote Sens Environ* 87: 470-481.

WILLSTATTER R & STOLL A. 1918. *Untersuchungen über die assimilation der kohlen-saure*, Berlin: Springer, 448 p.

YANG J, WEISBERG PJ & BRISTOW NA. 2012. Landsat remote sensing approaches for monitoring long-term tree cover dynamics in semi-arid woodlands: Comparison of vegetation indices and spectral mixture analysis. *Remote Sens Environ* 119: 62-71.

¹Programa de Pós-Graduação em Ecologia e Recursos Naturais, Departamento de Biologia, Campus do Pici, Universidade Federal do Ceará, Avenida Humberto Monte, s/n, 60440-900 Fortaleza, CE, Brazil

²Departamento de Biologia Vegetal, Instituto de Biologia, Rua Monteiro Lobato, 255, Universidade Estadual de Campinas – UNICAMP, 13083-862 Campinas, SP, Brazil

³Departamento de Engenharia Agrícola, Campus do Pici, Universidade Federal do Ceará, Avenida Humberto Monte, s/n, 60455-760 Fortaleza, CE, Brazil

⁴Laboratório de análise espacial, Centro de Investigaciones en Geografía Ambiental, Universidad Nacional Autónoma de México, Antigua Carretera a Pátzcuaro, 8701, Ex Hacienda San Jose de la Huerta, 58190 Morelia, Mich., México

⁵Divisão de Sensoriamento Remoto, Instituto Nacional de Pesquisas Espaciais, Avenida dos Astronautas, 1758, 12227-010, São José dos Campos, SP, Brazil

Programa de Pós-Graduação em Ecologia e Recursos Naturais, Departamento de Biologia, Campus do Pici, Universidade Federal do Ceará, Avenida Humberto Monte, s/n, 60440-900 Fortaleza, CE, Brazil

SUPPLEMENTARY MATERIAL

Table S1.

How to cite

DOS SANTOS TEIXEIRA A, MAS JF, MENEZES BS, PONZONI FJ & ARAÚJO FS. 2023. Landsat data respond to variations in the structure of Caatinga plant communities along a successional gradient. *An Acad Bras Cienc* 95: e20230022. DOI 10.1590/0001-3765202320230022.

FERNANDA KELLY G. DA SILVA¹
<https://orcid.org/0000-0002-4155-9412>

FERNANDO ROBERTO MARTINS²
<https://orcid.org/0000-0002-3068-7099>

ADUNIAS DOS SANTOS TEIXEIRA³
<https://orcid.org/0000-0002-1480-0944>

JEAN-FRANÇOIS MAS⁴
<https://orcid.org/0000-0002-6138-9879>

BRUNO S. DE MENEZES¹
<https://orcid.org/0000-0003-1134-8996>

FLAVIO JORGE PONZONI⁵
<https://orcid.org/0000-0001-5993-9053>

FRANCISCA S. DE ARAÚJO¹
<https://orcid.org/0000-0003-4661-6137>

Correspondence to: **Fernanda Kelly Gomes da Silva**
 E-mail: kelly.biologaeupb@hotmail.com

Author contributions

Conceptualization: Fernanda K. G. Silva, Fernando R. Martins, Adunias S. Teixeira, Francisca S. Araújo. Formal analysis: Fernanda K. G. Silva, Bruno S. Menezes, Adunias S. Teixeira, Jean-François Mas and Flavio Jorge Ponzoni Funding Acquisition: Francisca S. Araújo. Investigation; Visualization; Writing – original draft: Fernanda K. G. Silva Methodology: Fernanda K. G. Silva, Fernando R. Martins, Adunias S. Teixeira, Jean-François Mas. Supervision: Fernando R. Martins, Adunias S. Teixeira, Francisca S. Araújo. Writing – review & editing: Fernanda K. G. Silva, Fernando R. Martins, Adunias S. Teixeira, Jean-François Mas, Bruno S. Menezes, Francisca S. Araújo.

